

Impact of poloidal flux expansion on JET divertor radiation

B. VIOLA¹, G. Calabró¹, A. E. Jaervinen², I. Lupelli³, G. Rubino¹, S. Wiesen⁴, M. Wischmeier⁵
and JET EFDA Contributors *

EUROfusion Consortium, JET, Culham Centre of Fusion Energy, OX14 3DB Abingdon, UK

¹ *ENEA for EUROfusion, via E. Fermi 45, 00044 Frascati (Roma), Italy.*

² *Lawrence Livermore National Laboratory, Livermore, CA 94550, USA.*

³ *Culham Centre of Fusion Energy, OX14 3DB Abingdon, UK.*

⁴ *Forschungszentrum Jülich GmbH, Institut für Klima-und Energieforschung - Plasmaphysik,
52425 Jülich, Germany.*

⁵ *Max-Planck-Institut fuer Plasmaphysik, Boltzmannstr. 2, D-85748 Garching, Germany.*

Introduction

Divertor heat load and detachment control is mandatory in the next step devices, such as ITER, to maintain surface heat fluxes below $5 - 10 \text{ MW/m}^2$ and to minimize tungsten sputtering while operating at or above H_{98} of unity. Increasing divertor radiation by injecting low-Z impurities such as nitrogen or neon, to reduce scrape-off layer (SOL) heat flux and to cool the divertor plasma to detachment, is considered as the main tool to achieve this goal. An additional approach to handling the heat exhaust power is a strong flux flaring in a single divertor leg [1], [2]. A divertor with a strong flux flaring in a single divertor leg places the second X-point near the divertor plate, causing flared field lines there, which spreads the heat over a larger area and increases the line connection length. In this paper we will present results on the effects of poloidal flux expansion (FE) on radiation distribution and X-point peaking on JET ITER-like Wall (ILW) nitrogen seeded plasmas. Nitrogen seeded JET-ILW H-mode plasmas have been also investigated with EDGE2D-EIRENE [3]–[5], results of predictive simulations presented here [6] are compared with experimental data.

Experimental overview

The considered discharges are 2 MA, 2.15 T, $q_{95} = 3.35$ nitrogen seeded H-mode plasmas heated by 15MW of NBI power. Deuterium gas fuelling of $2.5 \times 10^{22} \text{ part/s}$ was applied through the high-field side (HFS) divertor base plate and the outer mid-plane gas injection modules (GIM), whereas nitrogen was applied through HFS divertor module only. The three discharges here analyzed differ only for the nitrogen seeding: zero (unseeded reference case), $1.2 \times 10^{22} \text{ part/s}$ and $3 \times 10^{22} \text{ part/s}$ JPN 91986, 92121 and 9213 respectively. We will refer to them as unseeded, low and high seeded case respectively. The upstream density and temperature profiles are measured by the High Resolution Thompson Scattering (HRTS) system and the downstreams by Langmuir probes. During current flat-top, divertor currents are changed in order to move a secondary X-point close to the inner divertor leg, thus increasing the magnetic poloidal flux expansion [7], both at the Xpoint and at inner and outer strike point. The

*See the author list of "X. Litaudon et al 2017 Nucl. Fusion 57 102001"

flaring of the magnetic flux (characterized by the magnetic field gradient) in the primary null is affected by the presence of the secondary null. This flaring could be then directly translated to the increased wetted surface area and reduced heat flux [2], [8]. Such high flux expansion (HFE) experimental discharges have been obtained at JET and compared to low flux expansion (LFE) ones as discussed in [9]. The magnetic topology that causes the poloidal spread of the power flow is generated by building a low $|B_{pol}|$ region surrounding the X-point much wider in the poloidal plane than the REF case. The flux map of the analyzed LFE and HFE cases is presented in [6] Fig. 1a, the red and blue contour, respectively. We derive a reduction factor for the heat load in the simple hypothesis that no dissipation takes place in the flow channel, so the total energy flow across a flux tube of width w has to be preserved, namely $q_{\parallel} w_{HFE} = q_{\parallel} w_{REF}$. Since $L_{\perp} \propto \tau_{dw}^{1/2} \propto L_c^{1/2}$ being L_c the total magnetic connection length and τ_{dw} the particle dwell time, we can pose $q_0 \Delta \Psi L_c^{1/2} |_{HFE} \sim q_0 \Delta \Psi L_c^{1/2} |_{REF}$. So we can expect an increase of divertor radiation equal to $f_r = (\Delta \Psi L_c^{1/2})_{HFE} / (\Delta \Psi L_c^{1/2})_{REF} = 1.22$

Modelling setup and experimental results

The simulation grid in this study corresponds to a modified version of low triangularity semi horizontal target typically used at JET, obtained by EFIT equilibrium code. The experimental density setup has been modelled as following: a feed-forward gas injection from private region and feedback density control from outer midplane (OMP) have been considered. Due to EFIT equilibrium uncertainties, a shift on the separatrix position of 2.8cm have been considered in HRTS profiles to reach upstream and LFS strike point electron pressure balance as predicted by two points model. Therefore, the upstream density profiles have been shifted on radial coordinate for the low density cases. A power flowing from the core to the SOL of 8 MW has been used in the simulations, as given by the total input power subtracted the core radiation with the 90% of the poloidal flux surface. A reasonable fit with HRTS [10] and Langmuir probes is obtained by assuming a particle diffusion coefficient $D_{\perp} = 0.15 m^2/s$ in the pedestal and near SOL region (i.e. up to $R_{sep} \pm 1cm$, where R_{sep} is the radial position of the separatrix at the low field side (LFS) midplane) and D_{\perp} nearly linearly increasing up to $3.5 m^2/s$ in the mid and far-SOL. The nitrogen content in the computational domain is feedback controlled to provide requested levels of nitrogen radiated power in the simulations: 0, 3, 5, and 6 MW. A model with cross field drifts omitted has been assumed for deuterium throughput. It should be noted that although deuterium throughput details (injection and pumping), with the given set of pumping surfaces and pumping albedos, are not expected to be fully taken into account, the relative discrepancy between the experiment and the model in the deuterium throughput does not change significantly during the nitrogen seeding scan. Once nitrogen is puffed in the domain, a factor of 2 increase is predicted in the LFS divertor radiated power, with the peak of the radiation distribution located in front of the target plate. Simultaneously, transition to high recycling conditions is observed at the LFS divertor as the peak electron temperature drops from 20eV to 10eV. Fig. 1 shows a comparison of the experimental inter-ELM bolometry profiles and EDGE2D/EIRENE predictions. An in-

crease of divertor radiation is experimentally observed and confirmed by EDGE2D simulated data for HFE case (see Figg. 1a and 1b). Whereas in the unseeded plasmas, the divertor radiation is underestimated in the EDGE2D/EIRENE simulations, by imposing the divertor radiation with nitrogen seeding, the measured radiated power levels and distribution in the divertor can be reproduced numerically in both configurations (Figg. 1c and 1d). It should be noted that, for the high seeding case, the measured radiated power in both divertor legs and simulated one are in good agreement. On the contrary, the simulated radiated power at the X-point is lower than the measured one and further analysis is needed. In both configurations, more than 90% of the total

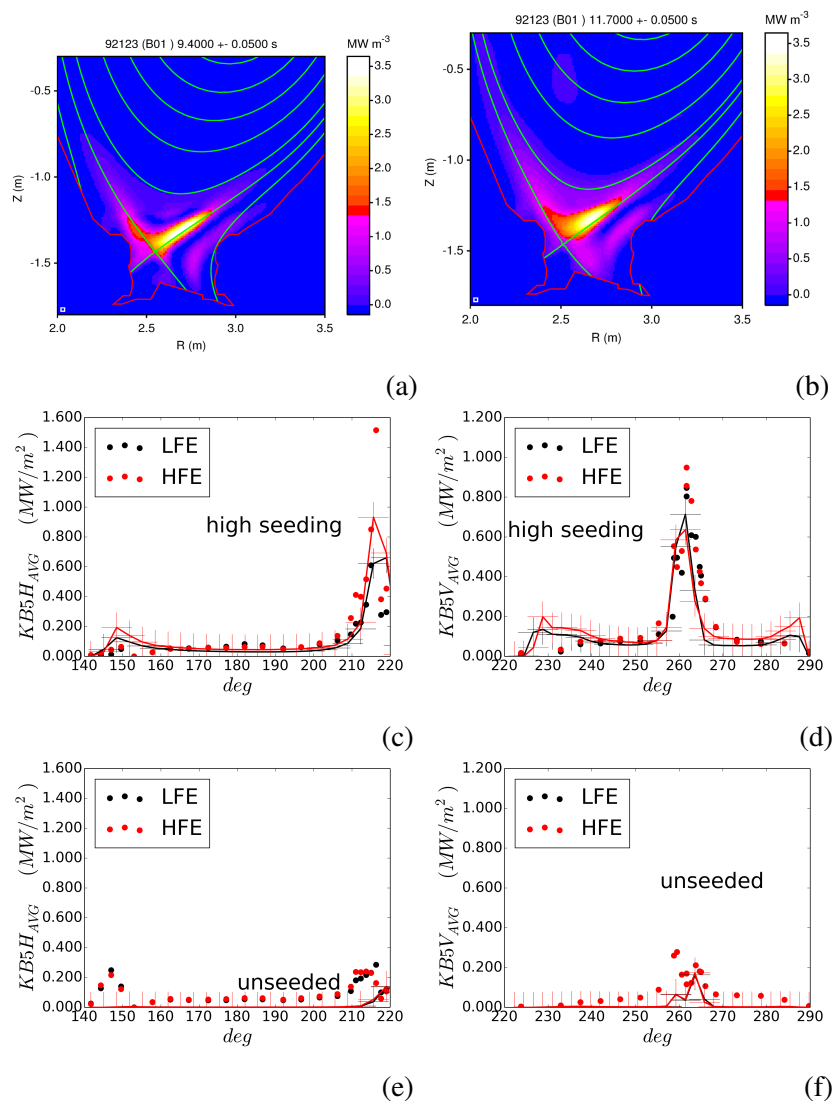


Fig. 1: (a) JPN 92123 low flux expansion time window, radiation pattern from the divertor bolometer; (b) JPN 92123 (highest level of seeding) high flux expansion time window, radiation pattern from the divertor bolometer; (c) and (d) predictions (solid lines) and experimental (dots) of the KB5 bolometer for JPN 92123: horizontal and vertical lines of sight, respectively; (e) and (f) predictions (solid lines) and experimental (dots) of the KB5 bolometer for JPN 91986 (unseeded case): horizontal and vertical lines of sight, respectively. Color code: red is the low flux expansion case, black is the high flux expansion case.

radiation in computational domain occurs outside the separatrix until a MARFE-like, radiation condensation formation is formed inside the X-point. Once this formation is present, most of the radiation occurs inside the separatrix in the simulations. Horizontal bolometer measurement for seeded case agree qualitatively with experiment, whereas for the unseeded case the code fails to reproduce the experimental data, predicting a low radiation. A detailed analysis of the power balance has been set up in order to physically investigate the reason of the increase of the radiated power for HFE discharges. Although the nitrogen radiation is constant in all the studied cases, the increase in the high flux expansion phase mainly does seem due to the molecular and charge exchange losses. As discussed in [11], an increase of charge exchange losses is mainly due to an increase of connection length and flux expansion both at X-point at strike point positions.

Conclusions

Interpretative EDGE2D-EIRENE code simulations have been set up to investigate radiative divertor operation in H-mode seeded low and high flux expansion discharges. Bolometry measurements have been compared with multi-fluid code predictions and are in qualitative agreement. Seeded cases are reasonably matched whereas the code is still unable to reproduce unseeded discharges.

Acknowledgments

This work has been carried out within the framework of the EUROfusion Consortium and has received funding from the Euratom research and training programme 2014-2018 under grant agreement No 633053. The views and opinions expressed herein do not necessarily reflect those of the European Commission.

References

- [1] R. Pitts et al., “Divertor geometry effects on detachment in TCV”, *Journal of Nuclear Materials*, vol. 290-293, pp. 940–946, 2001.
- [2] M. Kotschenreuther et al., “Magnetic geometry and physics of advanced divertors: The X-divertor and the snowflake”, *Phys. Plasmas*, vol. 20, no. 102507, 2010.
- [3] R. Simonini et al., *Contrib. Plasma Phys.*, vol. 34, pp. 368–373, 1994.
- [4] S. Wiesen et al., “EDGE2D/EIRENE code interface report”, Tech. Rep., 2006. [Online]. Available: http://www.eirene.de/e2deir_report_30jun06.pdf.
- [5] D. Reiter et al., “Progress in two-dimensional plasma edge modelling”, *Journal of Nuclear Materials*, vol. 196-198, pp. 80–89, 1992.
- [6] B. Viola et al., *Nuclear Materials and Energy*, 2017, submitted for publication.
- [7] V. A. Soukhanovskii et al., “Taming the plasma-material interface with the ‘snowflake’ divertor in NSTX”, *Nuclear Fusion*, vol. 51, no. 012001, 2011.
- [8] D. D. Ryutov et al., *Plasma Phys. Control. Fusion*, vol. 463, 2010.
- [9] G. Calabrò et al., *Proc. of the 22nd PSI conference on Plasma Surface Interaction, Rome, Italy, May 30th - June 3rd, 2016*, 2016.
- [10] L. Frassinetti et al., *Rev. Sci. Instrum.*, vol. 83, no. 013506, 2012.
- [11] G. Calabrò et al., *Nucl. Fusion*, vol. 55, no. 083005, 2015.
- [12] K. D. Lawson et al., *Nuclear Materials and Energy*, 2017, submitted for publication.